Research Article

Evaluation of Multispectral Sensors for Assessing Pigment Index in Soybean

Harman Singh Sangha[1]*, Ajay Sharda[1], William Schapaugh[2] and Dylan Walta[2]

[1]*Carl and Melinda Helwig Department of Biological and Agricultural Engineering, Kansas State University, USA*

[2]*Department of Agronomy, Kansas State University, USA*

*Corresponding Author: Harman Singh Sangha, Carl and Melinda Helwig Department of Biological and Agricultural Engineering, Kansas State University, USA.

Abstract

The collection of image-based data for vegetative crops is advancing with the introduction of vigorous and lightweight camera sensors. Among these camera sensors, multispectral sensors are prevalent with researchers due to the wide range of functions that can be performed. Multispectral sensors are carefully chosen according to their capacity to recognize specific wavelengths, and specifications such as focal length, sensor size, and radiometric resolution is often overlooked. Therefore, a study was performed to evaluate two forms of multispectral sensors for assessing pigment index by examining correlation between sensor output and ground parameters. A narrowband and broadband sensor was used to collect spectral data on a soybean field using a quadcopter. Spectral data was evaluated based on ground resolution, orthomosaic quality, along with statistical comparison with agronomical data (wilting scores and maturity). The broadband sensor had a better ability to capture comprehensive spatial data than the narrowband sensor. The broadband sensor was highly correlated with soybean maturity (r = 0.83, p ≤ 0.001). Wilting scores collected were of wide resolution as compared to spectral data. Narrow resolution ground data can verify that pigment index can be used as crop parameters. The Narrowband sensor was limited in estimating pigment index due to smaller sensor size and restricted spectral bands.

Keywords: Multispectral Sensors; Orthomosaic; Pigment-Index; Precision Agriculture

Abbreviations

PA: Precision Agriculture; UAS: Unmanned Aerial Systems; RGB: Red-Green-Blue; TIR: Thermal Infrared; CIR: Color Infrared; PI: Pigment Index; GNDVI: Green Normalized Difference Index; BNDVI: Blue Normalized Difference Index; GR: Ground Resolution; FP: Footprint

Introduction

There is a lot of pressure on agriculture to produce food for the ever-increasing human population [1]. The environment is often ignored to achieve this goal to reach higher efficiencies. The concept of sustainable agriculture has been introduced to avoid unwanted degradation of agricultural lands and conserve external inputs such as water, fertilizer, pesticides. A sustainable system should be resource-conserving, socially supportive, commercially competitive, and environmentally sound [2]. Precision agriculture (PA) contributes to creating a more sustainable agriculture environment. PA aims to optimize the use of resources to increase sustainability and profitability of agricultural systems by keeping environmental impact at a minimum and improving the quality of social aspects of agriculture [3]. PA provides tools and technologies to identify in-field soil and crop variability, offering a means to improve sub-field level farming practices and optimize agronomic inputs [4].

Remote Sensing plays a central role in attaining that goal by helping researchers determine in-field agricultural variation. Remote Sensing is done by measuring reflectance or emittance of electromagnetic waves, which are either reflected or produced by the plants after interacting with sunlight. Properties about a crop can be determined by observing these different wavelengths of light [5]. Designed primarily for military applications, unmanned aerial systems (UAS) are now used in agricultural scenarios as remote sensing platforms [6]. UAS provides an alternate option to traditionally used satellites and aircraft to collect data as they can minimize the influence from climatic variables, be flexible to use, and be economical compared to other remote sensing platforms [7]. Also, the data can be obtained in a higher resolution which could provide critical information for phenotyping studies on crops, disease detection, and crop stress evaluation [8-12].

With the development of robust and lightweight camera sensors, collecting remote sensing vegetative data in the field is rapidly evolving into standalone systems [8]. The use of UAS based sensors to detect water stress and quantify biomass in crops has been successfully demonstrated by many researchers [13-16]. The kind of information collected using remote Sensing depends on the type of sensor used, and sensor selection is based on the application in which it will be used. The sensor types can be classified broadly as Red-Green-Blue (RGB) sensors, thermal infrared (TIR) sensors, modified color infrared (CIR), narrowband multispectral sensors, and hyperspectral sensors [8,17-19].

Multispectral sensors are more popular among farmers and researchers compared to other UAS sensors since multispectral sensors provide information both in the visible and infrared spectrums [6]. Multispectral sensors can be divided into two categories, namely narrowband and broadband. A typical narrowband multispectral sensor has a bandwidth of 10 nm, whereas broadband sensors have a bandwidth range from 40 nm to 110 nm [20]. Both narrowband and broadband sensors can be used to estimate crop variables, but it is often found that information extracted from both sensors is neither in complete agreement nor conflict when compared with each other [21]. Usually, a multispectral sensor is selected based on the ability of the sensor to detect radiation from certain wavelengths, with specific configurations such as focal length, sensors size, bandwidth, and radiometric resolution not considered.

Considering the stated issue regarding camera selection for remote sensing purposes on UAS, this study was designed to compare and evaluate the performance of the two types of multispectral sensors commonly used in precision agriculture. The sensors were examined to assess differences in their ability to provide accurate remotely sensed data and derive a Pigment Index (PI) for soybean crop for multiple flights in the season. The multispectral sensory data was also compared to thermal infrared sensory data along with ground data collected during the season. In this study, the following objectives were set

- Compare and contrast the differences between PI values extracted from soybean and assess relative merits of PI derived from broadband and narrowband sensors to assess crop growth parameters.
- Check correlations between extracted data from remotely sensed imagery with ground data and thermal infrared sensory data collected during the soybean growing season.

Materials and Methods
sUAS and Cameras

A Matrice - 100 (DJI, Shenzhen, China) quadcopter was used to perform the aerial missions (Figure 1). The quadcopter could handle a maximum payload of 1 kilogram. The UAS was equipped with an in-built autopilot, and custom missions can be uploaded on the copter using third-party applications. It has dual battery compatibility; each battery provides 5700mAh power to the copter and provides 25 minutes of effective flight time with multispectral sensors (185-350 gms) onboard. The quadcopter can fly at wind speeds of up to 10 m/s. But to maintain safety standards and avoid error in data caused due to wind influence, data was collected when the wind speeds were less than 4.5 m/s. The sensors were mounted using a custom-made 3-D printed gimbal. The copter was used to collect color infrared imagery to compare multispectral. Cameras.

Two kinds of multispectral sensors were used: one was a narrowband sensor, Micasense Rededge-M (Micasense Inc., Seattle, WA, USA), with five bands of blue, green, red, red-edge, and near-infrared. The bandwidth varies from 10 nm to 40 nm for this sensor. The second sensor was a modified broadband infrared Sony α5100 (Sony Corporation of America, New York, NY). It had three bands of blue, green, and near infrared. Modified broadband cameras have broader bands than Micasense sensors close to 100 nm.

Figure 1: Matrice 100 quadcopter was used for infrared data collection.

The Micasense sensor had a global shutter, whereas Sony α5100 had a rolling shutter. Also, a Flir Vue pro R 13 mm (Flir Systems Inc, Wilsonville, OR USA) thermal infrared camera was used to collect thermal aerial imagery in °C temperature scale to cross verify the spectral response from both multispectral cameras (Figure 2). Thermal data was collected and calibrated using methods in [22].

Figure 2: Camera sensor used for this study: a) Micasense Rededge-M b) Flir Vue pro R 13 mm c) Sony α5100 modified CIR.

Crops and missions

Soybean was used for this study (Figure 3a). Data were collected for two consecutive years (2018 - 2019), with the different plot locations each year. Plot 'A' in 2018 was located south of Assaria, KS

(38.669030 N, -97.604247 W). In 2019, plot 'B' was located north of Assaria, KS (38.709675 N, -97.617792 W). The agronomic performance of Roundup Ready 2 Extend® commercial soybean cultivars was evaluated under dryland conditions as part of the Kansas Soybean Variety Performance Trials [23], [24]. Each cultivar was planted in 4-row plots with 3.70 m long rows, spaced 0.76 m apart. The experimental design was a randomized complete block with four replications. The planting rate was 30 seeds/ m. The soil type at plot 'A' site was a Detroit silty clay loam. The soil type at plot 'B' site was a Longford silt loam. There were 35 cultivars represented as E1, E2, etc., for 2018 and 31 cultivars for 2019. The missions were created on Mission Planner (Mission Planner®, by Michel Oborne) autopilot software suite. Mission Planner was used as a configuration utility and a dynamic control supplement for compatible autonomous vehicles. After determining the mission characteristics, the mission files were imported into a third-party autonomous flight application (Litchi® for DJI). The planned missions were then uploaded to the autopilot onboard the quadcopter, which carried out the missions and returned safely to the launch site. All missions were conducted at an altitude of 50 m, within ± 1.5 hours of solar noon, to avoid deep shadows and bidirectional reflectance artifacts. The quadcopter was flown at a velocity of 3 m/s for all missions. Multiple flights were done over the season, but only four days of good data collection were quantifiable (1: 08/02/2018, 2: 09/22/2018, 3: 09/03/2019, 4: 09/13/2019). The data from the sensors are abbreviated as the name of the sensor and code for the date of flight, e.g., RE1 for Rededge-M data. collected on 08/02/2018 and S3 for Sony α5100 data collected on 09/03/2019.
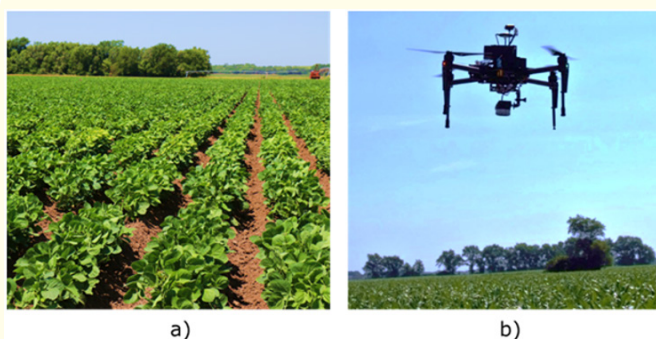

Figure 3: a) Soybean crop used for data collection b) Matrice 100 with a Sony α5100 CIR camera.

Ground data

Leaf wilting scores were collected on each plot on multiple days of the season [25]. Wilting scores were rated using a scale from 0-100. 0 represented no wilting, 20 represented slight wilting evidence and rolling of leaves at the top of the canopy, 40 represented severe rolling of leaves at the top of the canopy and moderated wilting of leaves throughout the plant, 60 represented severe wilting thought the canopy, 80 represented dead leaves throughout the canopy and severely wilted petioles and 100 represented plant death. The wilting scores collected four times during the 2018 season on 7/25, 08/01, 08/08, and 09/01/2018 and two times for the 2019 season on 09/06 and 09/16 will be abbreviated as W1, W2, W3, W4, W5, and W6, respectively. The most severe wilting scores were observed on 7/25 for the 2018 season. Scores for the latter three dates were relatively low because of more frequent rain events in the second half of the season. For the 2019 season, the plants did not show considerable wilting. Plant maturity was recorded as when 95% of soybean pods have reached stage R8 [26]. After maturity, the center two rows of each plot were harvested to measure seed yield (kg/ha).

Sensor comparison

The quality of data extracted from the sUAS imagery depends greatly on the quality of the images collected. Other factors which play a role in producing quality data are image overlap, flight time, calibration, etc. For qualitative and quantitative analysis for comparing the different multispectral sensors, the following experiments were performed with the aerial data collected

Ground resolution

Aerial and satellite imagery have ground resolution often listed as a parameter for comparing different sensors. According to [27], at least four pixels are required to detect the smallest feature in an image. Therefore, it becomes necessary to look at ground resolution for the imagery collected in this study to compare the two infrared sensors. The ground resolution and the footprint of the images collected for a flying altitude of 50 m were calculated for all the flights using ArcMap 10.4.1 (ArcGIS, ESRI, Redlands, CA, USA).

Statistical and orthomosaic analysis

One selected vegetative index was calculated using the infrared imagery from both sensors. A Pigment Index (PI) (Eq. – 3) was derived by subtracting the green normalized difference index (GNDVI) from the blue normalized difference index (BNDVI) (KSURF Invention Disclosure No.2016-010, 2016).

GNDVI = (NIR – Green)/(NIR + Green) -------(1)
BNDVI = (NIR – Blue)/(NIR + Blue) ------------(2)
PI = BNDVI – GNDVI -------------(3)
Where,
NIR = Near Infra-Red wavelength

During photosynthesis, plants produce reactive oxygen species as a secondary product along with sugars and fatty acids. High concentrations of reactive oxygen species are harmful to plants, and stress causes these concentrations to increase [13,28]. Also, fungi and bacteria produce reactive oxygen species to invade plant tissues. To reduce the concentration of reactive oxygen, plants produce carotenoids which behave as antioxidants [29]. Stress leads to higher carotenoid concentrations. Chlorophyll a and b absorb energy across blue and red regions of the electromagnetic spectrum, whereas carotenoids absorb photons in the blue and green regions [30], as seen in figure 4 [31]. Also, plants reflect a considerable amount of energy in the NIR region of the spectrum. BNDVI values are influenced by chlorophyll a and b content with some influence of carotenoids. GNDVI is influenced by carotenoid concentration to a larger extent and is used as a plant health indicator [32]. PI values indicate carotenoids to chlorophylls ratios; therefore, it is correlated with stress conditions in the plant and physiological reasons that lead to changes in chlorophyll-carotenoid ratios, such as plant progression through growth stages [33]. A major advantage of the PI compared to other spectral indices is that it decouples the influence of biomass from stress. Normalized Difference Vegetative

Index (NDVI) provides a high index. values even when the plant biomass is low. PI values are less influenced by biomass.

PI index was extracted from the orthomosaics generated for each 4-row plot, only selecting the middle two plots to avoid errors due to pixel mixing. The PI was averaged into a single value for each 4-row plot. ANOVA analysis was done to check the differences between cultivars and the sensor's ability to identify differences in cultivars. Cultivar means were used to check significant differences between cultivars with respect to yield, maturity, S1, S2, RE1, RE2, F1, W1, W2, W3, and W4 for the year 2018 and yield, maturity, S3, S4, RE3, RE4, W5 and W6 for the year 2019. Thermal imagery was not collected in the second year due to the unavailability of the
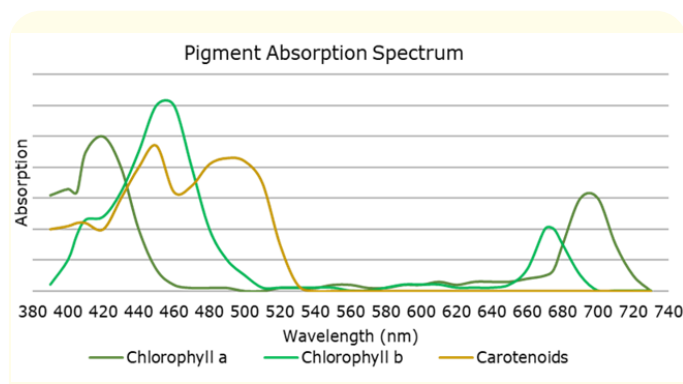
Figure 4: Plant Pigment spectral absorption distribution

Figure 5: Ground resolution comparison for
a) Sony α5100 CIR and b) Rededge-M.

sensor. A correlation matrix was created for checking the overall correlations between ground and aerial data (R Foundation, USA).

Results and Discussion
Ground resolution and spectral discrimination

The ground resolution (GR) and foot-print (FP) from both the infrared sensors were calculated for a mission altitude of 50 m. The GR and FP for Sony α5100 with 16 mm focal length were GR = 1.22 cm and FP = 73.4 x 48.8 m, whereas for Rededge-M with focal length 5.5 mm, GR = 3.47 cm and FP = 44.4 x 33.3 m. The Sony α5100 provides better ground resolution and foot-print than Rededge-M, which means more information is available from the imagery for calculating PI values (Figure 5). Also, there was a vast difference in sensor size between the Sony α5100 and Rededge-M. The Sony α5100 had a sensor size of 23.5 x 15.6 mm with 6000 x 4000 pixels on the sensor array. The Rededge-M had a sensor size of 4.8 x 3.6 mm with 1280 x 960 pixels on the sensor array. Rededge-M is a wide-angle camera (focal length = 5.4 mm) as compared to Sony α5100 (focal length = 16 mm). Sony α5100 16 mm lens is a less sharp lens; due to this, there are more pixels for transition between the two gradients. The results exhibited that Sony α5100 had better capability to gather more detailed spatial information of the crop canopy to calculate more accurate PI values. Rededge-M collected imagery in 16-bit (65,536 value intervals) radiometric resolution while the Sony α5100 imagery was collected with 8-bit (256 value intervals) radiometric resolution.

Statistical orthomosaic analysis

The orthomosaics created during this study were compared (Figure 6). The orthomosaics were created for the entire field,
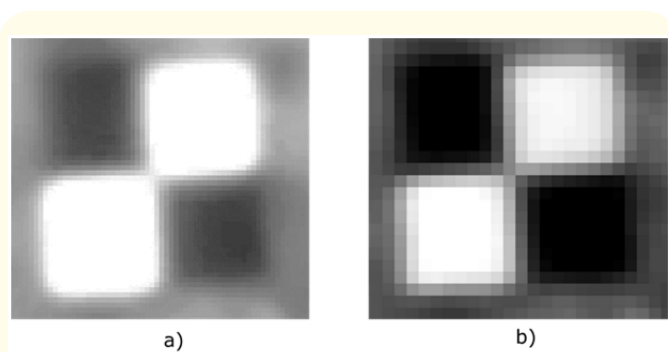
not limited to the cultivars used for comparison. Similar patterns were found between imagery collected from S2, RE2, and F2 for 2018. The pattern does not necessarily represent the cultivar differences. The areas in the close-up section of crop marked with the red boundary were areas where the plots spectrally exhibited poor health, and areas marked with the green boundary were the areas that exhibited good health. These patterns indicated that even though different sensors were used in this study, the spectral response of all the sensors remained similar. Further statistical comparison between camera sensors and ground data was done to fully evaluate the performance of the sensors.

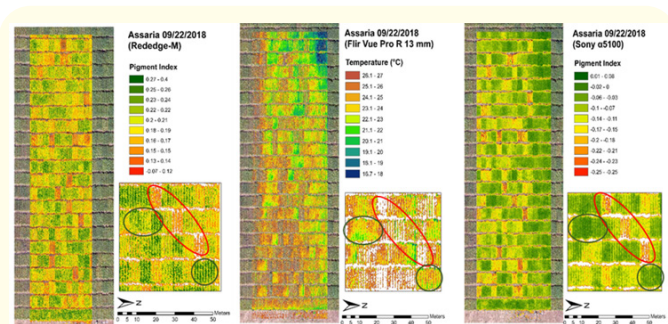**Figure 6:** Orthomosaic generated with infrared
imagery used in this study.

Table 1 shows the F-values from analyses of variance for cultivar differences with respect to yield, maturity, S1, S2, RE1, RE2, F1, W1, W2, W3, and W4 for the year 2018. Maturity S2, RE2, and W2 exhibited larger cultivar differences than the other variables. A correlation matrix (along with significance levels) was created to

evaluate the relationship between the phenotypic variables evaluated for cultivars (Tables 2 and 3). S2 was highly correlated with maturity (r = 0.83, p ≤ 0.001). S2 was also correlated with yield (r = 0.49, p ≤ 0.01). RE2 was only found to be significantly correlated to yield (r = 0.63, p ≤ 0.001). Part of the correlation of S2 and RE2 with yield is due to later stages of crop maturity. Chlorophyll concentration decreases during senescing, and stress is no longer is the rea-son for reduced chlorophyll activity [34]. F2 showed a correlation with maturity and S2 with r values of -0.68 (p ≤ 0.001) and -0.61 (p ≤ 0.001), respectively. The correlation between S1 with maturity and RE1 with S1 and S2 was significant but turned out to be small. S1 was found to correlate with maturity (r = 0.47, p ≤ 0.01). RE1 was correlated to S1 and S2 with r values of 0.47 (p ≤ 0.01) and 0.43 (p ≤ 0.05) respectively.

	Y	Maturity	S1	S2	RE1	RE2
F-values	3.465***	60.762***	7.683***	59.415***	6.026***	30.077***
	F2	W1	W2	W3	W4	
F-values	2.956***	10.8***	15.514***	2.029**	2.998***	
SIGNIF. CODES: '***' 0.001, '**' 0.01, '*' 0.05, '.' 0.1, '' 1						

Table 1: Analysis of variance summary for cultivar difference for the year 2018.

Entry	Yield	Maturity	S1	S2	RE1	RE2	F2	W1	W2	W3	W4
E1	3104.5	27.5	-0.023	-0.143	0.071	0.191	23.2	36	3	11	14
E2	3388.9	29	-0.009	-0.105	0.080	0.219	23.7	33	3	10	9
E3	3628.7	30.25	-0.034	-0.110	0.066	0.220	24.1	31	14	15	21
E4	3172.4	28.75	-0.048	-0.100	0.068	0.205	23.7	51	34	23	18
E5	3543.6	34.75	-0.029	-0.052	0.074	0.235	22.9	41	13	13	13
E6	3595.5	38	-0.016	-0.043	0.090	0.206	22.8	43	25	19	15
E7	3657.1	41	-0.031	-0.057	0.081	0.189	22.0	29	11	9	18
E8	3129.1	25	-0.050	-0.139	0.072	0.191	23.7	36	14	18	9
E9	3717.8	37	-0.020	-0.042	0.101	0.226	23.8	55	48	18	24
E10	3039.9	46.5	-0.018	-0.027	0.055	0.146	21.6	-	-	-	3
E11	3509.9	28.75	-0.027	-0.064	0.077	0.238	23.9	46	30	23	28
E12	3352.9	41	-0.030	-0.063	0.085	0.190	22.5	26	11	9	21
E13	3063.9	26.25	-0.018	-0.154	0.070	0.188	23.4	28	0	9	18
E14	3672.0	32.25	-0.032	-0.107	0.075	0.229	25.3	36	13	14	29
E15	3698.8	29	-0.053	-0.085	0.059	0.215	23.1	50	41	19	33
E16	3433.0	29.75	-0.030	-0.068	0.089	0.231	24.0	49	33	20	15
E17	3174.0	32.25	-0.046	-0.096	0.081	0.235	24.6	41	18	19	26
E18	3443.9	41.5	-0.017	-0.047	0.088	0.183	21.5	63	48	19	33
E19	3570.1	32.5	-0.031	-0.098	0.084	0.234	24.4	36	13	13	33
E20	3622.8	33.75	-0.024	-0.055	0.076	0.235	23.3	45	11	11	10
E21	3774.8	40.75	-0.020	-0.041	0.089	0.202	22.8	35	16	16	33
E22	4027.3	35.75	-0.016	-0.041	0.078	0.244	21.8	35	13	11	16
E23	3642.1	29.5	-0.050	-0.096	0.074	0.215	23.0	49	18	19	39
E24	3380.2	27	-0.047	-0.124	0.069	0.199	23.9	41	24	15	35
E25	3309.4	27.5	-0.029	-0.140	0.074	0.192	25.1	23	3	11	31

E26	3457.5	28	-0.026	-0.135	0.078	0.192	24.4	20	1	9	20
E27	3663.8	27.25	-0.034	-0.140	0.060	0.196	24.2	23	6	9	20
E28	3581.6	32	-0.035	-0.066	0.069	0.231	23.0	53	35	17	28
E29	4105.8	35.25	-0.014	-0.054	0.090	0.246	23.8	45	26	11	36
E30	3957.5	35	-0.030	-0.045	0.081	0.245	22.0	31	18	11	20
E31	3762.1	40.5	-0.018	-0.026	0.082	0.228	22.7	28	5	18	18
E32	3572.2	38.75	-0.035	-0.048	0.082	0.222	23.3	54	38	20	31
E33	3651.0	35.75	-0.025	-0.052	0.076	0.230	23.7	35	26	13	16
E34	3772.7	28.5	-0.050	-0.086	0.062	0.212	24.6	55	43	19	23
E35	3511.0	39.75	-0.025	-0.063	0.082	0.199	22.0	23	5	10	10
Mean	3533.92	33.314	-0.030	-0.080	0.077	0.213	23.37	38.8	19.1	14.6	21.7
Variance	136332.4	31.052	0.000199	0.001464	0.000149	0.000546	2.59	154.2	228.7	46.0	169.0
CV	7.93	4.23	-28.69	-12.18	10.59	3.85	4.83	17.00	36.75	41.45	49.64
LSD (0.05)	393.08	1.979	0.0119	0.0137	0.01140	0.01151	1.58	9.3	9.9	8.5	15.1

Table 2: Main effects means table for all the variables for the year 2018.

	Maturity	S1	S2	RE1	RE2	F2	W1	W2	W3	W4
Yield	0.24	0.15	0.49 **	0.31.	0.63 ***	-0.1	0.09	0.22	-0.08	0.33.
Maturity		0.47 **	0.83 ***	0.39 *	-0.14	-0.68 ***	0.06	0.16	-0.05	-0.13
S1			0.37 *	0.47 **	0	-0.34 *	-0.23	-0.27	-0.42 *	-0.31.
S2				0.43 *	0.28	-0.61 ***	0.35 *	0.42 *	0.24	-0.08
RE1					0.34 *	-0.11	0.15	0.18	0.05	0.19
RE2						0.24	0.25	0.2	0.18	0.23
F2							-0.05	-0.04	0.11	0.3.
W1								0.88 ***	0.74 ***	0.34.
W2									0.72 ***	0.38.
W3										0.3.
Signif. codes: '***' 0.001, '**' 0.01, '*' 0.05, '.' 0.1, ' ' 1										

Table 3: Correlation matrix for cultivar data of year 2018.

Significant correlations were observed between the wilting scores and the sensor data, but the correlations tended to be small and varied in sign (Table 3.) For example, a positive association was observed between W2 and S2 (r = 0.42, p ≤ 0.05), while a negative association was observed between W3 and S1 (r = -0.42, p ≤ 0.05). One possible reason for this inconsistency may have been related to the timing of the measurements. S2 was recorded later in the growing season than W2 when the plants began to mature. S1 and W3 were recorded within six days of each other during pod fill and

resulted in an expected negative correlation between PI and wilting, where cultivars with less wilting and under less stress tended to have higher PI values. However, in this data set, wilting scores were limited to discern differences among the cultivars and were not correlated to seed yield.

Table 4 shows the F-values from analyses of variance for cultivar differences with respect to yield, maturity, S3, S4, RE3, RE4, W5, and W6 in 2019. Maturity, RE3, and RE4 exhibited larger cultivar

differences than the other variables. A correlation matrix (along with significance levels) was created to evaluate the relationship between the phenotypic variables evaluated for cultivars (Tables 5 and 6). S3 and S4 were found to be highly correlated with maturity ($r = 0.58$, $p \leq 0.001$ and 0.58, $p \leq 0.001$ respectively). S3 was also correlated with S4 ($r = 0.94$, $p \leq 0.01$). RE4 was significantly negatively correlated to maturity ($r = -0.59$, $p \leq 0.001$). W6 was negatively correlated with Maturity ($r = -0.64$, $p \leq 0.001$).

	Yield	Maturity	S3	S4	RE3	RE4
F-values	6.6113***	57.1627***	5.2154***	5.0211***	24.538***	28.3295***
	W5	W6				
F-values	2.7879***	1.6107.				
SIGNIF. CODES: '***' 0.001, '**' 0.01, '*' 0.05, '.' 0.1, '' 1						

Table 4: Analysis of variance summary for cultivar difference for the year 2019.

Entry	Yield	Maturity	S3	S4	RE3	RE4	W5	W6
E1	4428.2	28.25	-0.003	-0.021	0.176	0.250	4.5	NA
E11	4140.2	29	0.003	-0.022	0.162	0.214	3.8	37.5
E12	3868.7	29	0.002	-0.029	0.176	0.203	6.3	35.0
E13	4353.4	34.5	0.022	-0.013	0.176	0.198	16.3	35.0
E19	4029.3	28.75	-0.004	-0.034	0.196	0.246	2.5	30.0
E2	4095.4	30.25	-0.006	-0.034	0.154	0.193	2.5	33.8
E20	4355.6	29	-0.001	-0.025	0.164	0.202	12.0	36.3
E21	4227.7	29.75	0.009	-0.019	0.184	0.217	3.8	36.3
E22	4275.1	29	0.023	0.000	0.204	0.265	2.5	45.0
E23	4275.8	29.25	0.001	-0.021	0.205	0.265	11.3	35.0
E24	4158.9	29	-0.004	-0.029	0.191	0.249	1.3	25.0
E25	3965.9	39.75	0.014	-0.007	0.173	0.186	7.5	22.5
E26	4104.4	35.25	0.006	-0.018	0.187	0.227	2.5	28.3
E27	4207.8	29.75	-0.005	-0.027	0.210	0.274	5.0	NA
E28	4118.7	29.5	-0.011	-0.039	0.162	0.199	8.8	37.5
E29	4173.4	34.75	0.013	-0.010	0.184	0.217	1.3	26.3
E3	3526.6	28.25	-0.022	-0.046	0.187	0.241	1.3	NA
E30	4054.7	29.25	-0.013	-0.043	0.162	0.199	8.8	33.3
E31	4135.0	35.25	0.014	-0.008	0.173	0.184	3.8	26.3
E32	4160.9	36.75	0.013	-0.011	0.170	0.189	0.0	18.8
E33	3908.2	34.5	0.008	-0.012	0.174	0.189	8.8	31.3
E34	3726.5	37.5	0.015	-0.010	0.182	0.197	2.5	28.8
E35	3100.1	40.5	0.005	-0.025	0.162	0.167	1.3	23.8
E37	4047.1	29	-0.017	-0.049	0.202	0.251	1.3	NA
E38	3891.6	35.25	-0.003	-0.018	0.183	0.213	13.3	35.0
E39	4169.7	38.5	0.007	-0.016	0.170	0.191	12.5	26.3

E4	4150.8	28.75	-0.021	-0.044	0.169	0.205	0.0	30.0
E44	4394.5	29.25	0.005	-0.019	0.187	0.252	5.0	NA
E45	4386.0	28.75	-0.009	-0.039	0.161	0.208	1.3	30.0
E46	4271.0	29	-0.002	-0.024	0.181	0.210	3.8	30.0
E54	4195.9	29.75	-0.012	-0.042	0.163	0.197	12.5	37.5
Mean	4093.5	31.77	0.001	-0.024	0.178	0.216	5.4	30.9
Variance	72846.7	14.9	0.000133	0.000167	0.000216	0.000794	20.4	32.6
CV	5.1	3.2	1158.2	-47.5	3.3	4.9	100.3	26.0
LSD	601.5	2.92	0.029	0.033	0.017	0.0303	15.5	-

Table 5: Main effects means table for all the variables for the year 2019.

	Maturity	**S3**	**S4**	**RE3**	**RE4**	**W5**	**W6**
Yield	-0.46 *	0.09	0.11	0.11	0.35.	0.22	0.33
Maturity		0.58 ***	0.58 ***	-0.2	-0.59 ***	0.12	-0.64 ***
S3			0.94 ***	0.11	-0.19	0.12	-0.14
S4				0.17	-0.11	0.12	-0.17
RE3					0.83 ***	-0.15	0.12
RE4						-0.18	0.4 *
W5							0.38.
Signif. codes: '***' 0.001 '**' 0.01 '*' 0.05 '.' 0.1 ' ' 1							

Table 6: Correlation matrix for cultivar data of year 2019.

Rededge-M was limited in its ability to calculate PI values. For fully observing the carotenoid activity with respect to chlorophyll, broad coverage of each color spectrum is required. The chlorophyll and carotenoid overlapping electromagnetic spectrum activity were discussed in the methods. Sony α5100 being a broadband camera had overlapping bands and sensed the full region in which the pigments are active. The Rededge-M senses a narrow region in the spectrum and no overlap between the bands. Rededge-M is therefore, does not fully capture the pigment absorption spectrum for carotenoids.

Conclusion

Sony α5100 displayed the better capability to gather more detailed spatial information of the crop canopy to calculate PI. Overall ANOVA and LSD means exhibited that the cultivars displayed maximum differences in means for maturity, S2, RE2, and W2 for the year 2018 and 2019 for yield, maturity, S3, S4, RE3, RE4, W5, and W6. S2 was found highly correlated to maturity (r = 0.83, p ≤ 0.001). Also, S3 and S4 were found to be correlated with maturity (r = 0.58, p ≤ 0.001 and 0.58, p ≤ 0.001 respectively). Wilting scores were found limited in their ability to provide higher resolution data than spectral data. The spectral responses can be confirmed as an actual crop parameter with better resolution ground data. Rededge-M was discovered to be restricted in calculating the PI due to sensor limitations. In future studies, other vegetative indices derived from Rededge-M bands will be examined to check whether they correlate with cropping parameters and ground data.

Conflict of Interest

The authors don't have any conflict of interest.

Bibliography

1. MC Hunter., *et al.* "Agriculture in 2050: Recalibrating Targets for Sustainable Intensification". *Bioscience* 386.4 (2017).

2. R Duesterhaus. "The SWCS view: Sustainability's promise". *Journal of Soil and Water Conservation* 45.1 (1990): 4.

3. R Gebbers and VI Adamchuk. "Precision Agriculture and Food Security". *Science* 327.5967 (2010): 828-831.

4. S Khanal., *et al.* "An overview of current and potential applications of thermal remote sensing in precision agriculture". *Computers and Electronics in Agriculture* 139. Elsevier B.V (2017): 22-32.

5. A Mac Arthur and I Robinson. "A critique of field spectroscopy and the challenges and opportunities it presents for remote sensing for agriculture, ecosystems, and hydrology". in Remote Sensing for Agriculture, Ecosystems, and Hydrology XVII 9637 (2015): 963705.

6. JD Rudd., *et al.* "Application of satellite, unmanned aircraft system, and ground-based sensor data for precision agriculture: A review" (2017).

7. C Zhang., *et al.* "The application of small unmanned aerial systems for precision agriculture: a review". *Precis. Agric* 13 (2012): 693-712.

8. JAJ Berni., *et al.* "Thermal and narrowband multispectral remote sensing for vegetation monitoring from an unmanned aerial vehicle". *IEEE Transactions on Geoscience and Remote Sensing* 47.3 (2009): 722-738.

9. J Baluja., *et al.* "Assessment of vineyard water status variability by thermal and multispectral imagery using an unmanned aerial vehicle (UAV)". *Irrigation Science* 30.6 (2012): 511-522.

10. S Candiago., *et al.* "Evaluating multispectral images and vegetation indices for precision farming applications from UAV images". *Remote Sensing* 7.4 (2015): 4026-4047.

11. M Zaman-Allah., *et al.* "Unmanned aerial platform-based multi-spectral imaging for field phenotyping of maize". *Plant Methods* 11.1 (2015): 1-10.

12. J Senthilnath., *et al.* "Application of UAV imaging platform for vegetation analysis based on spectral-spatial methods". *Computers and Electronics in Agriculture* 140 (2017): 8-24.

13. J Bendig., *et al.* "Combining UAV-based plant height from crop surface models, visible, and near infrared vegetation indices for biomass monitoring in barley". *The International Journal of Applied Earth Observation and Geoinformation* 39 (2015): 79-87.

14. S Park., *et al.* "Estimation of crop water stress in a nectarine orchard using high-resolution imagery from unmanned aerial vehicle (UAV)". in Proceedings of the 21st International Congress on Modelling and Simulation, Gold Coast, Australia (2015): 29.

15. S Park., *et al.* "Dependence of CWSI-Based Plant Water Stress Estimation with Diurnal Acquisition Times in a Nectarine Orchard". *Remote Sensing* 13.14 (2021): 2775.

16. M Awais., *et al.* "UAV-based remote sensing in plant stress imagine using high-resolution thermal sensor for digital agriculture practices: a meta-review". *International Journal of Environmental Science and Technology* 2021 (2022): 1-18.

17. D Kingston and R Beard. "Real-time attitude and position estimation for small UAVs using low-cost sensors". in AIAA 3rd" Unmanned Unlimited" Technical Conference, Workshop and Exhibit (2004): 6488.

18. B Majidi and A Bab-Hadiashar. "Real time aerial natural image interpretation for autonomous ranger drone navigation". in Digital Image Computing: Techniques and Applications (DICTA'05) (2005): 65.

19. PJ Zarco-Tejada., *et al.* "Assessing vineyard condition with hyperspectral indices: Leaf and canopy reflectance simulation in a row-structured discontinuous canopy". *Remote Sensing of Environment* 99.3 (2005): 271-287.

20. L Deng., *et al.* "UAV-based multispectral remote sensing for precision agriculture: A comparison between different cameras". *ISPRS Journal of Photogrammetry and Remote Sensing* 146 (2018): 124-136.

21. D Zhao., *et al.* "A comparative analysis of broadband and narrowband derived vegetation indices in predicting LAI and CCD of a cotton canopy". *ISPRS Journal of Photogrammetry and Remote Sensing* 62.1 (2007): 25-33.

22. HS Sangha., *et al.* "Impact of camera focal length and sUAS flying altitude on spatial crop canopy temperature evaluation". *Computers and Electronics in Agriculture* 172 (2020): 105344.

23. KSRE. "2018 Kansas Performance Tests with soybean varieties". Report of Progress 1146. Manhattan (2018).

24. KSRE. "2019 Kansas Performance Tests with soybean varieties". Report of Progress 1153. Manhattan (2019).

25. CA King., *et al.* "Differential wilting among soybean genotypes in response to water deficit". *Crop Science* 49.1 (2009): 290-298.

26. WR Fehr., *et al.* "Stage of development descriptions for soybeans, Glycine Max (L.) Merrill 1". *Crop Science* 11.6 (1971): 929-931.

27. T Hengl. "Finding the right pixel size". *Computational Geosciences* 32.9 (2006): 1283-1298.

28. BER Hodecker., *et al.* "Water availability preceding long-term drought defines the tolerance of Eucalyptus to water restriction". *New For* 49.2 (2018): 173-195.

29. SH Kim., *et al.* "Down-regulation of β-carotene hydroxylase increases β-carotene and total carotenoids enhancing salt stress tolerance in transgenic cultured cells of sweetpotato". *Phytochemistry* 74 (2012): 69-78.

30. EW Chappelle., *et al.* "Ratio analysis of reflectance spectra (RARS): an algorithm for the remote estimation of the concentrations of chlorophyll a, chlorophyll b, and carotenoids in soybean leaves". *Remote Sensing of Environment* 39.3 (1992): 239-247.

31. Heliospectra. "LED light spectrum 101: Absorption spectra" (2014).

32. AA Gitelson., *et al.* "Use of a green channel in remote sensing of global vegetation from EOS-MODIS". *Remote Sensing of Environment* 58.3 (1996): 289-298.

33. NM Hatton. "Use of small unmanned aerial system for validation of sudden death syndrome in soybean through multispectral and thermal remote sensing". *Environmental Science* (2018).

34. C Lu and J Zhang. "Changes in photosystem II function during senescence of wheat leaves". *Physiologia Plantarum* 104.2 (1998): 239-247.